

# Importance of Intracellular Water Apparent Diffusion to the Measurement of Membrane Permeability

Jonathan V. Sehy,\* Alison A. Banks,<sup>‡</sup> Joseph J. H. Ackerman,<sup>†§¶</sup> and Jeffrey J. Neil<sup>§¶</sup>

\*Program in Molecular Cell Biology and †Department of Chemistry, Washington University, St. Louis, Missouri 63130, ‡Department of Biology, Bowdoin College, Brunswick, Maine 04011, §Departments of Radiology and ¶Internal Medicine, Washington University School of Medicine, St. Louis, Missouri 63110, and ¶Departments of Neurology and Pediatrics, St. Louis Children's Hospital, St. Louis, Missouri 63110 USA

**ABSTRACT** The exchange of water across biological membranes is of fundamental significance to both animal and plant physiology. Diffusional membrane permeability ( $P_d$ ) for the *Xenopus* oocyte, an important model system for water channel investigation, is typically calculated from intracellular water pre-exchange lifetime, cell volume, and cell surface area. There is debate, however, whether intracellular water motion affects water lifetime, and thereby  $P_d$ . Mathematical modeling of water transport is problematic because the intracellular water diffusion rate constant ( $D$ ) for cells is usually unknown. The measured permeability may be referred to as the *apparent* diffusional permeability,  $P'_d$ , to acknowledge this potential error. Herein, we show that magnetic resonance (MR) spectroscopy can be used to measure oocyte water exchange with greater temporal resolution and higher signal-to-noise ratio than other methods. MR imaging can be used to assess both oocyte geometry and intracellular water diffusion for the same single cells. MR imaging is used to confirm the dependence of intracellular water lifetime on intracellular diffusion. A model is presented to relate intracellular lifetime to true membrane diffusional permeability. True water diffusional permeability ( $2.7 \pm 0.4 \mu\text{m/s}$ ) is shown to be  $39 \pm 6\%$  greater than apparent diffusional permeability for 8 oocytes. This discrepancy increases with cell size and permeability (such as after water channel expression) and decreases with increasing intracellular water  $D$ .

## INTRODUCTION

The *Xenopus* oocyte is the principal mRNA expression system for the investigation of translated membrane receptor and channel proteins. As such, it is an important model system for the measurement of plasma membrane water permeability. Water permeability for the oocyte (or any cell) is described by two indexes, each of which may be affected by separate factors. Diffusional permeability ( $P_d$ ) is determined by monitoring the exchange of labeled water between the cell and its surroundings. Osmotic permeability ( $P_f$ ) relies on the measurement of rate of cell volume change during an osmotic challenge. The permeability values measured in these two ways are often not equivalent, with  $P_f$  being somewhat greater than  $P_d$ .

There are two main interpretations for a ratio of  $P_f/P_d > 1$ . First, a high  $P_f$  may suggest the presence of water channels in the plasma membrane (Koefoed-Johnsen and Ussing, 1953). This criterion was used to propose the existence of pores in cell membranes before the existence of water channels was proven. Second,  $P_d$  may be underestimated due to the dependence of membrane water exchange on intracellular water motion. If intracellular water is relatively slow in reaching the cell membrane, passage through the membrane may not be the rate-limiting step in exchange of water between the cell and

its surroundings. The measured diffusional permeability may be referred to as the apparent  $P_d$  ( $P'_d$ ) to acknowledge this potential problem.

Many studies have attempted to address the possible dependence of  $P'_d$  on intracellular water motion (Lovtrup, 1963; Barry and Diamond, 1984; Finkelstein, 1987). Mathematical modeling of water transport has been hindered because the magnitude of intracellular water displacement over time is typically unknown. We have recently reported measurements of the water apparent diffusion coefficient (ADC) in the *Xenopus* oocyte (Sehy et al., 2001, 2002a, b). The ADC is a measure of displacement over time that reflects not just fluid-phase diffusion, but also the effects of barriers (i.e., intracellular membranes and macromolecules) and intermolecular binding on water displacement.

This report details the use of magnetic resonance (MR) in the quantification of diffusional membrane permeability for the *Xenopus* oocyte. Magnetic resonance spectroscopy is used to monitor membrane water exchange with better temporal resolution and signal-to-noise ratio (SNR) than previously described methods. Oocyte geometry is quantified from high-resolution three-dimensional (3D) MRI. From these two parameters, the apparent diffusional permeability  $P'_d$  is calculated with comparison to values from other techniques. Time course MRI is used to confirm the dependence of water exchange on intracellular water motion for the oocyte. The relationship between the true and apparent diffusional permeabilities is discussed in depth, incorporating recent measurements of the oocyte intracellular water ADC.

Submitted April 12, 2002 and accepted for publication July 12, 2002.

Address reprint requests to Jeffrey J. Neil, MD, PhD, Biomedical MR Laboratory, Campus Box 8227, Washington University School of Medicine, 4525 Scott Ave. Rm. 2313, St. Louis, MO 63110. Tel.: 314-362-9995; Fax: 314-362-0526; E-mail: neil@wuchem.wustl.edu.

© 2002 by the Biophysical Society

0006-3495/02/11/2856/08 \$2.00

## MATERIALS AND METHODS

### Oocyte dissection

Portions of ovary were dissected from mature female *Xenopus laevis* (Xenopus Express, Homosassa, FL), anesthetized by immersion in 1 g/l 3-aminobenzoic acid ethyl ester (Smith et al. 1991). Defolliculated stage V oocytes were isolated from ovarian tissue after 4 h of digestion with 0.2 mg/ml type I collagenase (Sigma, St. Louis, MO) in  $\text{Ca}^{2+}$ -free media (98 mM NaCl, 2.0 mM KCl, 1.0 mM  $\text{MgCl}_2$ , 5.0 mM HEPES pH 7.5, 2.5 mM sodium pyruvate, 50 units/ml penicillin, 0.05 mg/ml streptomycin). Oocytes were stored in  $\text{Ca}^{2+}$ -containing media (96 mM NaCl, 1.8 mM  $\text{CaCl}_2$ ) at room temperature not more than three days prior to use. Healthy oocytes were selected under a dissecting microscope by morphology and pigmentation.

### MR measurements of water exchange

All image and spectroscopy data were collected at room temperature (23°C) in a 4.7-T Oxford Instruments magnet equipped with a 600 mT/m Magnex gradient set and a Varian (San Fernando, CA)<sup>UNITY</sup> INOVA console. Oocytes were individually positioned in capillary tubing of inside diameter 1.6 mm. Oocytes were perfused with  $\text{Ca}^{2+}$ -containing media at 0.3 ml/h. A 2-mm-diameter solenoid tuned and matched to the  $^1\text{H}$  frequency acted as the radio-frequency (RF) transmitter/receiver. Cell volume was measured before beginning water exchange experiments. Three dimensional image data were collected with a microscopy-modified 3D spin-echo sequence (Sehy et al., 2001) (repetition time (TR) = 0.5 s, echo time (TE) = 66 ms) with voxel size of  $(50 \mu\text{m})^3$ . The image set was collected with a long TE to provide optimum contrast between media and cytoplasm, which differ greatly in  $T_2$  relaxation (Sehy et al. 2001). Surface area was calculated from cell volume assuming a spherical geometry.

To measure the apparent diffusional water permeability  $P_d'$  of the oocyte,  $\text{Ca}^{2+}$ -containing media formulated in deuterium oxide ( $^2\text{H}_2\text{O}$ ) was flowed at 1.5 ml/min past individual cells in the  $^1\text{H}$  RF coil (Note that the media average velocity was calculated to be 12 mm/s in the capillary and increased to 23 mm/s in moving around the oocyte). The signal-sensitive length of the RF coil/antenna was  $\sim 3$  mm). A simple pulse-and-collect sequence (TR = 0.5 s, acquisition time = 0.16 s) was used to measure the relative  $^1\text{H}_2\text{O}$  content of the cell during total exchange with  $^2\text{H}_2\text{O}$ -formulated media. Time points collected before the  $^2\text{H}_2\text{O}$  wave front passed through the coil were discarded. Time course data were fit to the equation,

$$S(t) = S(0)e^{-t/\tau} + B, \quad (1)$$

where  $S(t)$  is the relative  $^1\text{H}_2\text{O}$  content inside the cell at time  $t$ . A constant,  $B$ , was added to the right side of Eq. 1 to account for nondecaying background signal intensity from intracellular lipid methine  $^1\text{H}$  nuclei whose resonance frequency coincides with that of  $^1\text{H}_2\text{O}$ . The time constant  $\tau$  is the intracellular pre-exchange lifetime (inverse of the exchange rate constant) described by

$$\tau = \frac{V}{P_d'A}, \quad (2)$$

where  $V$  is the cell volume, and  $A$  is the cell surface area. All values are reported as mean  $\pm$  standard deviation.

After measurement of cell volume (35 min) and cell water exchange (10 min), oocytes were re-equilibrated with  $^1\text{H}_2\text{O}$ -formulated media. To determine whether water exchange across the membrane is limited by intracellular displacement to the site of exchange, a time course of  $^1\text{H}$  two-dimensional (2D) spin-echo images (TR = 0.35 s, TE = 6.3 ms, individual image time = 11.2 s) was obtained during total exchange with  $^2\text{H}_2\text{O}$ -formulated media. A single 0.25-mm imaging slice was positioned down the center of the cell parallel to the vegetal-animal axis. In-plane resolution

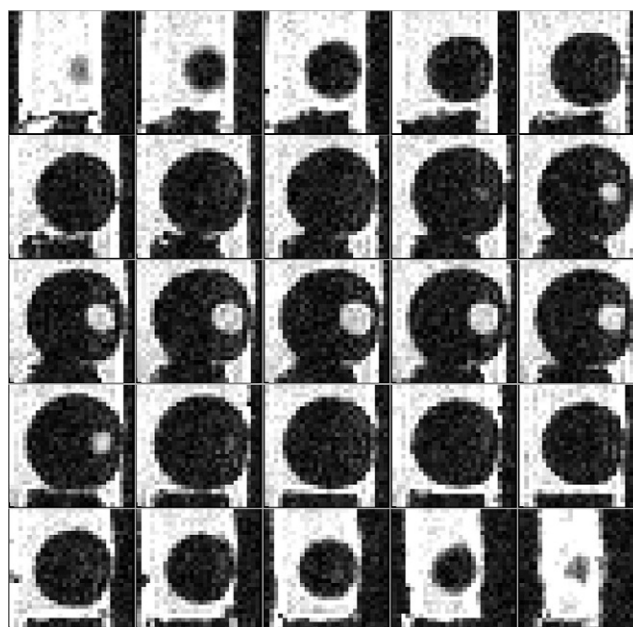


FIGURE 1  $T_2$ -weighted high-resolution 3D MRI of an oocyte. The figure is oriented such that the oocyte rests atop a polyurethane stopper in a vertically oriented capillary. Image sets like these were used to measure oocyte volume. Note that volumes corresponding to media and nucleus show high intensity due to long water  $T_2$ . The volume corresponding to cytoplasm shows low intensity similar to noise due to short water  $T_2$ . Volume measured for 8 oocytes from such images was  $0.84 \pm 0.03 \mu\text{l}$ .

was  $(0.25 \text{ mm})^2$ . The time course of signal intensity decay for each image voxel was fitted by Eq. 1. If water mixing within the cell were fast compared to exchange across the membrane, the time constant  $\tau$  for water signal decay would be expected to be independent of location within the cell. If water mixing within the cell were slow compared to exchange across the membrane,  $\tau$  would be expected to be longer in the center of the cell than in volumes nearer to the membrane.

### MR measurement of intracellular apparent diffusion

For qualitative comparison to water-exchange time-constant maps, ADC maps were constructed. High-resolution 3D spin-echo MRI data (TR = 0.5 s, TE = 14.8 ms,  $\delta$  = 3.9 ms,  $\Delta$  = 4.7 ms, voxel size =  $\{60 \mu\text{m}\}^3$ , image matrix =  $128 \times 64 \times 64$ ) were collected for the oocyte at two diffusion weightings ( $b_1 = 22 \text{ s/mm}^2$ ,  $b_2 = 1,020 \text{ s/mm}^2$ ). Diffusion weighting was incremented by increasing the amplitude of a magnetic-field gradient pair flanking the  $\pi$  pulse (Stejskal and Tanner 1965). The water ADC for each voxel was calculated according to

$$\text{ADC} = \frac{-\ln(S_2/S_1)}{b_2 - b_1}, \quad (3)$$

where  $S_i$  is the voxel intensity from the  $i$ th image.

## RESULTS

Figure 1, a sequential series of 2D slices, shows a representative high-resolution 3D MRI of an oocyte. Volume measured for the 8 oocytes from such images was  $0.84 \pm 0.03$

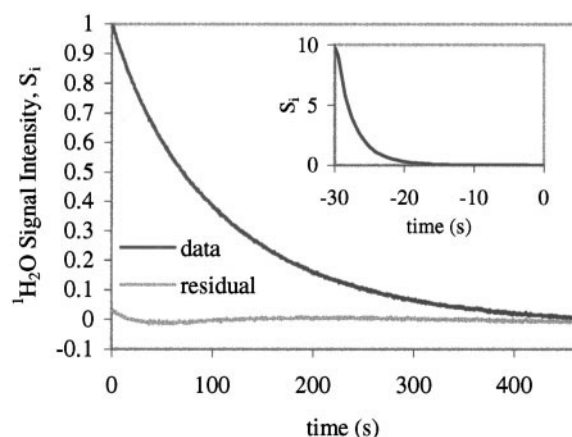


FIGURE 2 Decay of intracellular  $^1\text{H}_2\text{O}$  during replacement by  $^2\text{H}_2\text{O}$  from perfusing  $^2\text{H}_2\text{O}$ -formulated media. The residual from a monoexponential curve fit by Eq. 1 is plotted below the data. Note that adjacent data points overlap due to the high temporal resolution (0.5 s/point) of the MR measurement. The constant  $B$  representing nondecaying background signal was  $< 1\%$  of  $S(0)$ . Water intracellular pre-exchange lifetime  $t$  for 8 oocytes was  $103 \pm 12$  s. *Inset:* Decay of  $^1\text{H}_2\text{O}$  during replacement by  $^2\text{H}_2\text{O}$  with no oocyte present in the RF coil. From this plot, the time required for passage of the  $^2\text{H}_2\text{O}$  front can be ascertained. Time  $t = 0$  represents the point at which data collection would typically begin. At  $t = 0$ ,  $^1\text{H}_2\text{O}$  content in the empty RF coil was  $< 2\%$  of  $^1\text{H}_2\text{O}$  content in the RF coil containing the oocyte.

$\mu\text{l}$ . Surface area was  $4.3 \pm 0.1 \text{ mm}^2$ . Figure 2 shows a representative time course for  $^1\text{H}_2\text{O}$  residence in a follicle-free oocyte during total exchange with extracellular  $^2\text{H}_2\text{O}$ . The residual signal from a fit of Eq. 1 to the MR spectroscopy data is plotted below the data time course. Water intracellular pre-exchange lifetime,  $\tau$ , for 8 oocytes was  $103 \pm 12$  s. Apparent water permeability,  $P'_d$ , which was independently calculated for each oocyte from  $\tau$ , volume, and surface area using Eq. 2, was  $1.9 \pm 0.2 \mu\text{m/s}$ .

MRI  $^1\text{H}_2\text{O}$  content time courses were collected to give a spatially dependent measure of  $^1\text{H}_2\text{O}$  residence over time for the oocyte during total exchange with extracellular  $^2\text{H}_2\text{O}$ . Signal intensity for each voxel was fit by Eq. 1 to yield a distinct time constant. If water motion within the oocyte were fast compared to exchange across the membrane, the time constant for  $^1\text{H}_2\text{O}$  content loss in different volumes of the oocyte would be expected to be the same. Figure 3 A shows time-constant maps for 7 oocytes. The average time constant map is shown in Fig. 3 B. Figure 3 C compares these results with a representative map of the water ADC. The average time-constant map shows two trends. First, the time constant for  $^1\text{H}_2\text{O}$  content loss is longer in volumes near the center of the oocyte than in volumes near the border of the oocyte. Second, the time constant is longer in volumes with a relatively low ADC. For example, in Fig. 3 B, the volume with the longest time constant is in the vegetal hemisphere, just to the left of the midline. Figure 3 C shows that the vegetal hemisphere has

a relatively low water ADC. If the water ADC were not spatially dependent, the volume with longest time constant in Fig. 3 B would be expected to be centered within the cell.

## DISCUSSION

### Measurement of apparent diffusion permeability

This study details the measurement of intracellular water pre-exchange lifetime for the *Xenopus* oocyte by MR spectroscopy. From this water lifetime and measurements of oocyte geometry, which was quantified from high-resolution MRI,  $P'_d$  was calculated. Table 1 compares these results with measurements of  $P'_d$  from other studies.

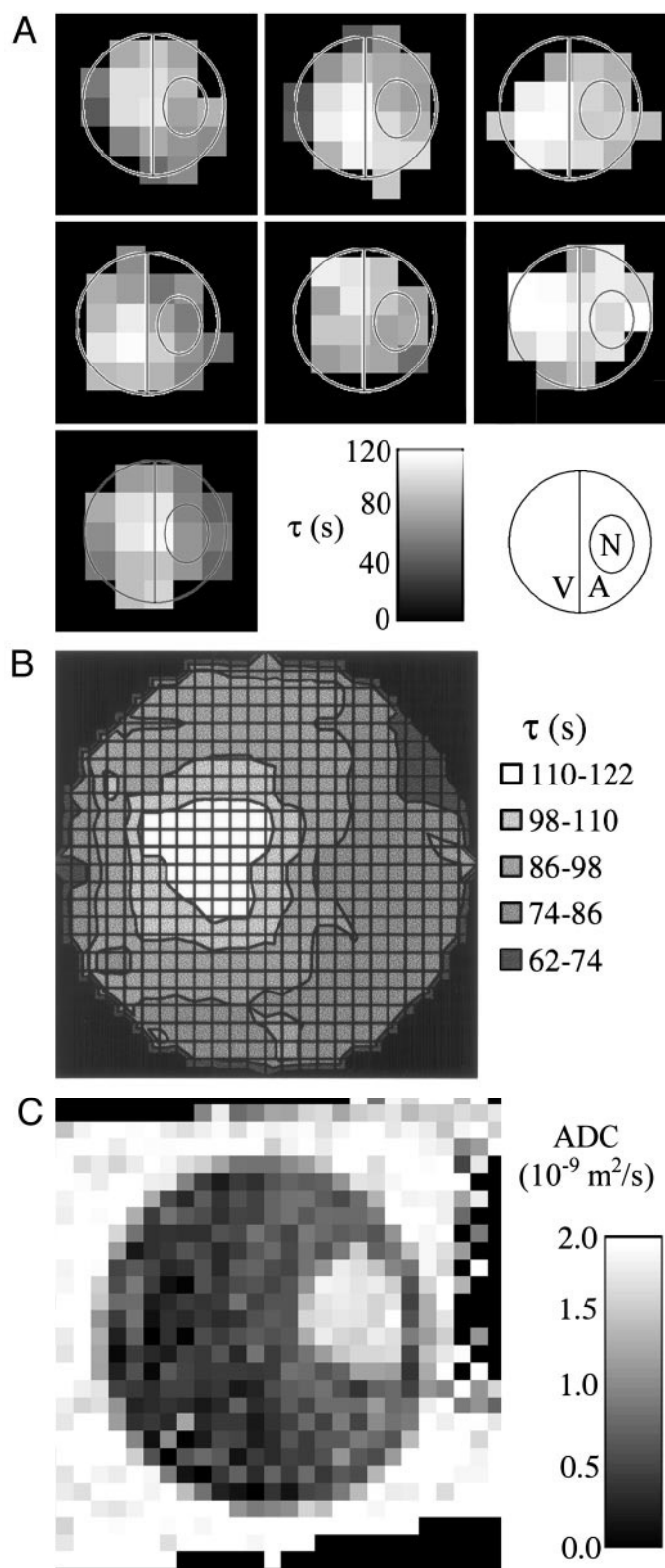
The time course for water exchange in the oocyte is typically measured by monitoring the efflux of tritium-labeled water ( $^3\text{H}_2\text{O}$ ) from either one oocyte or a collection of oocytes. Oocyte(s) are equilibrated in labeled media and transferred to a rapidly mixed volume of unlabeled media. Aliquots are then taken from the bathing media over time, and the amount of  $^3\text{H}_2\text{O}$  washed out is measured by scintillation counting. These experiments typically fit an intracellular lifetime to data from 10 or fewer time points (Zhang and Verkman, 1991; Iserovich et al., 1997). In contrast, the MR lifetime measurement depicted in Fig. 2 for a single oocyte incorporated data from almost 1000 time points. The small random scatter in residual data indicates that the data had a relatively high SNR.

Measurements of oocyte water exchange using  $^2\text{H}_2\text{O}$  were popular decades ago, before enriched  $^3\text{H}_2\text{O}$  was readily available. Typically, those methods involved the measurement of oocyte mass with the Cartesian diver balance as  $^1\text{H}_2\text{O}$  and  $^2\text{H}_2\text{O}$  exchanged across the cell membrane (Prescott and Zeuthen, 1952). Those experiments tended to yield longer water intracellular lifetimes than more recent studies, possibly as a result of inadequate mixing of extracellular media. Strong mixing is required to maintain a large diffusion gradient across the cell membrane. However, strong mixing tends to perturb the oocyte and thereby disrupt measurements of oocyte mass. In comparison to data from the MR technique described herein, data from that method suffers from relatively low SNR and temporal resolution. More recently, another technique monitoring oocyte water exchange using  $^2\text{H}_2\text{O}$  was reported (Iserovich et al., 1997). In that method, intracellular lifetime was derived from "flotation time" (the time that an  $^1\text{H}_2\text{O}$ -equilibrated oocyte will float in  $^2\text{H}_2\text{O}$  before beginning to sink). The study authors stress the qualitative aspects of that simple technique. They suggest it could be used to rapidly confirm water channel mRNA expression.

Up to this point, discussion of the measurement of  $P'_d$  has been confined to studies involving the oocyte, but the methods described above are equally applicable to any relatively large cell. With increasingly smaller cells, however, other techniques may be required because water intracellular life-



FIGURE 3 (A) Oocyte maps of the time constant  $\tau$  for  $^1\text{H}_2\text{O}$  content loss. A time course of 2D spin-echo images (voxel size =  $\{0.25 \text{ mm}\}^3$ , individual image time = 11.2 s) was obtained during total exchange of intracellular  $^1\text{H}_2\text{O}$  with extracellular  $^2\text{H}_2\text{O}$  (total time = 500 s). The time course of signal intensity loss for each image voxel was fitted by Eq. 1 (voxels with initial signal intensity below a threshold value were discarded). Geographical indicators were added to the relatively low-resolution time-constant maps based on high-resolution scout images. A, animal hemisphere; V, vegetal hemisphere; N, nucleus. The terms “animal” and “vegetal” designate volumes defined by surface coloring. The two hemispheres differ in many properties, including protein and lipid content. See Sehy et al. (2001). (B) Contour map of average time constant  $\tau$  for  $^1\text{H}_2\text{O}$  content loss. The seven time constant maps from Fig. 3 A were coregistered on a high-resolution grid ( $5\times$  in both dimensions), and time constant values were averaged for each grid element. (C) Oocyte water ADC map. Voxel size =  $(60 \mu\text{m})^3$ . The distribution of water ADCs in the oocyte has been previously reported (Sehy et al., 2001). The water ADC is higher in the animal hemisphere (which includes the nucleus) than in the vegetal hemisphere. This difference is related to the lipid and protein distributions within the cell; concentrations of lipid and protein decrease in moving from the animal pole to the vegetal pole. Interestingly, Fig. 3 B shows that the  $^1\text{H}_2\text{O}$  content-loss time constant for 7 oocytes was lower in the animal hemisphere than in the vegetal hemisphere. The water  $D$  representative of the oocyte was reported to be  $0.9 \times 10^{-9} \text{ m}^2/\text{s}$  (Sehy et al., 2002c).



time becomes too short for straightforward analysis. For reviews of these techniques (including NMR methods), the reader is referred to Herbst and Goldstein (1989) and Verk-

man (2000). Results from MRI experiments shown in Fig. 3 suggest that intracellular water diffusion may be important to the measurement of water exchange across the oocyte cell

**TABLE 1** Apparent diffusional membrane permeability

$P_d'$ ( $\mu\text{m/s}$ )	Label	Detection Parameter	Temperature ( $^{\circ}\text{C}$ )	Reference
$1.9 \pm 0.2$ (SD)*	$^2\text{H}_2\text{O}$	$^1\text{H}$ NMR	23	Present study
$2.0 \pm 0.3$ (SE)	$^2\text{H}_2\text{O}$	Mass	4	Iserovich et al., 1997
$2.2 \pm 0.2$ (SE)	$^2\text{H}_2\text{O}$	Mass	10	Iserovich et al., 1997
$2.0 \pm 0.1$ (SE)	$^3\text{H}_2\text{O}$	Radioactivity	10	Iserovich et al., 1997
$1.5 \pm 0.2$ (SE)	$^3\text{H}_2\text{O}$	Radioactivity	4	Zhang and Verkman, 1991
$3.4 \pm 0.2$ (SE)	$^3\text{H}_2\text{O}$	Radioactivity	25	Zhang and Verkman, 1991

\*True permeability  $P_d$  was  $2.7 \pm 0.4 \mu\text{m/s}$ .

membrane. A discussion of the relationship between  $D$  and  $P_d$  follows. First, exchange is considered for a freely permeable spherical cell with finite intracellular water diffusion. Second, exchange is considered for a spherical cell with finite intracellular water diffusion and finite membrane permeability. Using a model relating  $D$  and  $\tau$  to  $P_d$ , values of  $P_d$  for the oocyte are reported.

### Diffusion from a freely permeable spherical cell

The equations describing diffusion from a sphere have long been known, and their derivations can be found elsewhere (Carslaw and Jaeger, 1959; Lovtrup, 1963; Mild, 1972; Crank, 1975). Some of those expressions are discussed here.

Diffusion in a sphere (e.g., a cell with no membrane) can be described by

$$\frac{\partial u}{\partial t} = D \frac{\partial^2 u}{\partial r^2}, \quad (4)$$

where  $D$  is the diffusion coefficient,  $r$  is the distance from the center of the sphere, and  $u = c \cdot r$ , where  $c$  is the concentration of diffusing substance. It has been shown herein that MR can measure the exchange of  $^1\text{H}_2\text{O}$  for  $^2\text{H}_2\text{O}$  in the oocyte. Let it be assumed that  $c = 0$  outside the cell and that at  $t = 0$ ,  $c = c_0$  inside the cell. The solution of Eq. 4, describing the diffusion out of a sphere with radius  $R$ , for which no diffusion barrier (membrane) exists at the surface, must satisfy the following conditions:

$$u = c_0 \cdot r \quad 0 \leq r \leq R \quad t = 0, \quad (5)$$

$$u = 0 \quad r > R \quad t \geq 0, \quad (6)$$

$$u = f(r) \cdot r \quad 0 \leq r \leq R \quad t > 0. \quad (7)$$

With these conditions, diffusing substance in the sphere as a function of time can be described by

$$S(t) = S(0) \cdot \frac{6}{\pi^2} \sum_{n=1}^{\infty} \frac{1}{n^2} e^{-Dn^2\pi^2t/R^2}. \quad (8)$$

At long time  $t$ , this equation can be simplified to the first term of the series (i.e.,  $n = 1$ , see Fig. 4) to yield Eq. 1, where now,

$$\tau = \frac{R^2}{D\pi^2}. \quad (9)$$

We have recently reported the intracellular water ADC of the oocyte; it was  $0.9 \times 10^{-9} \text{ m}^2/\text{s}$  (Sehy et al., 2002c). Note that this single ADC value is effectively the average ADC value for all water in the oocyte. Figure 5 A depicts water intracellular pre-exchange lifetime (calculated from Eq. 9 using  $D = 0.9 \times 10^{-9} \text{ m}^2/\text{s}$ ) for a freely permeable spherical cell as a function of radius. A freely permeable sphere with a volume of  $0.84 \mu\text{l}$  (the mean volume of the oocytes used herein) would exhibit a water pre-exchange lifetime of 39 s due to finite intracellular diffusion alone. Mean lifetime measured from 8 oocytes was 103 s. Although not greatly higher, this suggests nevertheless that finite intracellular diffusion increases lifetime. The inset to Fig. 5 A gives lifetime for a freely permeable spherical cell as a function of radius for much smaller cells. Lifetimes of 6–22 ms have been reported for red blood cells, which are shaped like biconcave disks (Herbst and Goldstein, 1989).

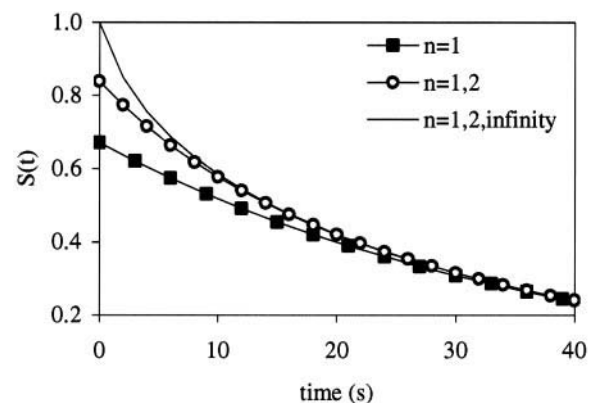


**FIGURE 4** Water in a freely permeable sphere (volume =  $0.84 \mu\text{l}$ ,  $D = 0.9 \times 10^{-9} \text{ m}^2/\text{s}$ ) as a function of time can be described by an infinite series (Eq. 8). This graph compares  $S(t)$  of the infinite series to  $S(t)$  when the series is approximated by either one or two terms. After 30 s, the first term of the series is 98% of the sum of the infinite series.

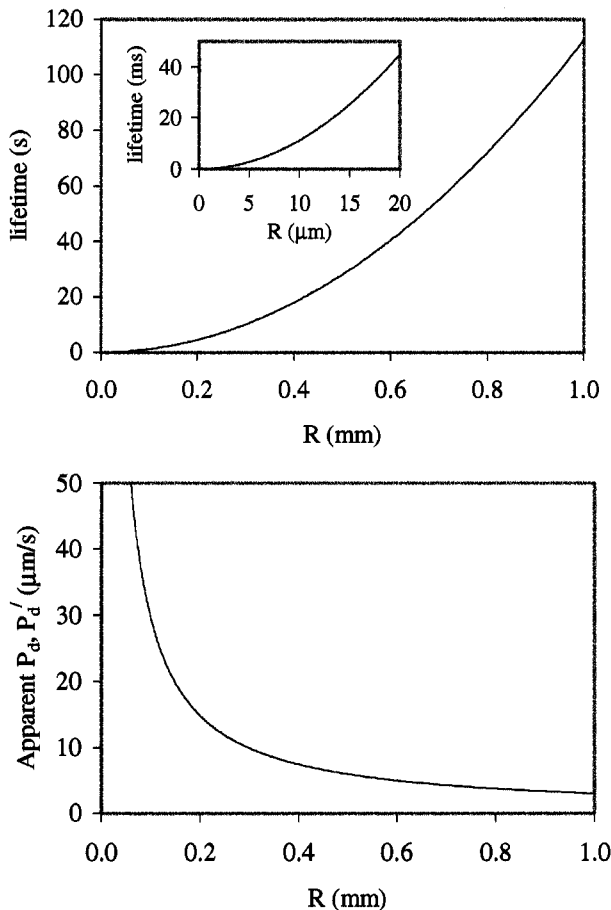


FIGURE 5 (A) Intracellular water pre-exchange lifetime for a freely permeable spherical cell as a function of radius, where  $D = 0.9 \times 10^{-9} \text{ m}^2/\text{s}$ . *Inset:* Lifetime as a function of radius for smaller cells. (B) Apparent diffusional permeability  $P'_d$  for a freely permeable spherical cell as a function of radius where  $D = 0.9 \times 10^{-9} \text{ m}^2/\text{s}$ .

Comparing these values to the lifetimes of spheres with radii of  $\sim 2\text{--}3 \text{ } \mu\text{m}$  suggests that lifetime is determined almost exclusively by membrane permeability in these cells.

Figure 5 B shows  $P'_d$ , calculated by rearrangement of Eq. 2, for freely permeable spheres as a function of radius, where  $D$  was assumed to be  $0.9 \times 10^{-9} \text{ m}^2/\text{s}$  and lifetime was calculated from Eq. 9. Note that  $P'_d$  decreases as radius increases, and intracellular diffusion becomes more important in governing the exchange process. For a freely permeable sphere of  $0.84 \text{ } \mu\text{l}$  (the volume of the oocytes used herein),  $P'_d$  due to finite diffusion alone (i.e.,  $D = 0.9 \times 10^{-9} \text{ m}^2/\text{s}$ ) would be  $5.1 \text{ } \mu\text{m/s}$ . It has been shown that treatment of oocytes with increasing amounts of amphotericin (a pore-forming compound) increases  $P'_d$  to a limiting value (Iserovich et al., 1997). Treatment of oocytes with  $500 \text{ } \mu\text{g/ml}$  amphotericin yields a  $P'_d$  of  $5.1 \pm 0.5 \text{ } \mu\text{m/s}$  at  $25^\circ\text{C}$  (Zhang and Verkman, 1991). The similarity of this result to the predicted  $P'_d$  for a freely permeable sphere supports the model.

### Diffusion from a spherical cell with finite membrane permeability

If a diffusion barrier (membrane) surrounds the sphere, the boundary condition,

$$-D \frac{\partial c}{\partial r} = P_d \cdot c_r \quad r = R, \quad (10)$$

is imposed on Eq. 4. This condition states that the amount of substance leaving the sphere equals the true diffusional permeability constant  $P_d$  times the concentration difference between the two sides of the surface. The concentration just within the surface is  $c_R$ , and on the outside it is assumed to be zero. The solution to Eq. 4 is now

$$S(t) = S(0) \sum_{n=1}^{\infty} \frac{6L^2 e^{-\beta_n^2 D t / R^2}}{\beta_n^2 [\beta_n^2 + L(L-1)]}, \quad (11)$$

where  $\beta_n$  are the roots of the equation,

$$\beta_n = (1-L) \tan \beta_n \quad (12)$$

and

$$L = \frac{R \cdot P_d}{D}. \quad (13)$$

At long time  $t$ , Eq. 11 can be simplified to the first term of the series (the value of the infinite series in Eq. 11 converges more rapidly to the value of the first term of the series with increasing  $t$  than the series in Eq. 8) to yield Eq. 1, where now

$$\tau = \frac{R^2}{\beta_1^2 D}. \quad (14)$$

When no permeability barrier exists at the surface,  $P_d$  and  $L$  are each equal to  $\infty$ , and  $\beta_n = n\pi$ . Insertion of these values into Eq. 11 simplifies it to Eq. 8.

Figure 6 shows calculated  $P_d$  as a function of  $D$  for a sphere with volume  $0.84 \text{ } \mu\text{l}$  and water lifetime of  $103 \text{ s}$  (the mean volume and lifetime for the oocytes used herein). As  $D$  increases,  $P_d$  approaches  $P'_d$ . As  $P_d$  increases,  $D$  approaches the value that yields a water lifetime of  $103 \text{ s}$  from a freely permeable sphere. Some studies have attempted to measure  $D$  from large cells using a relationship similar to that depicted in Fig. 6 by treating cells with agents assumed to greatly increase  $P_d$  (Haglund and Loeffler, 1969). Using  $0.9 \times 10^{-9} \text{ m}^2/\text{s}$  for  $D$  (Sehy et al., 2002c),  $P_d$  is  $2.7 \pm 0.4 \text{ } \mu\text{m/s}$ ,  $39 \pm 6\%$  greater than  $P'_d$ .

It is important to note that the fit of Eq. 1 to water exchange data in Fig. 2 has some systematic error (residual data are correlated). This error may be because  $c_0$  and  $D$  are not constant within the cell (Sehy et al., 2001) as was assumed in the models described above. A more complicated model describing water lifetime and its relationship to

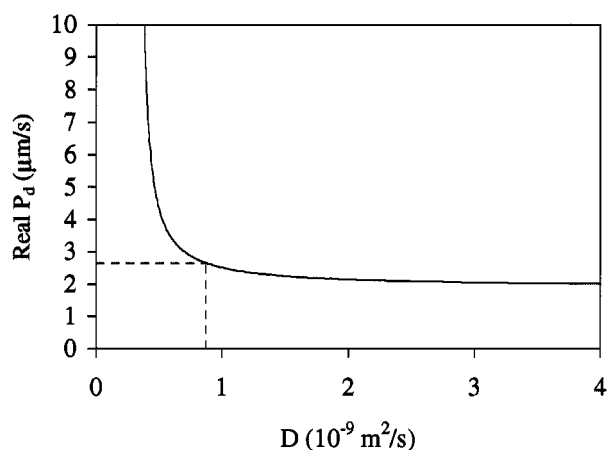


FIGURE 6 True diffusional permeability  $P_d$  as a function of  $D$  for a spherical cell of volume  $0.84 \mu\text{l}$  and water lifetime of 103 s. These values are the mean volume and lifetime for the 8 oocytes reported herein. The apparent diffusional permeability  $P'_d$  for these oocytes was  $1.9 \pm 0.2 \mu\text{m/s}$ . The dotted lines give the actual  $P_d$  and  $D$  for these oocytes.

permeability that takes into account these inhomogeneities may better fit the data. Note that the error was not predominantly due to the simplification of fitting only the first term of the series in Eq. 11 to the data. Data were collected beginning 30 s after the onset of water exchange, at which point the value of the first term differs from the value of the infinite series by  $<2\%$ .

### Other models relating $P_d$ and $D$

Some investigators have used other expressions to account for the possible dependence of  $P'_d$  on  $D$  in diffusional permeability studies. Waldeck, et al. argued that water exchange is not diffusion limited in a spherical cell as long as  $3D\tau/R^2 > 1$  (Snaar and Van As, 1992; Waldeck et al., 1995). Using values discussed herein for the oocyte,  $3D\tau/R^2 = 0.8$ . This result is consistent with our conclusion that intracellular diffusion affects water exchange in this system. However, discussion of the dependence of  $P'_d$  on  $D$  in terms of a limit may be an oversimplification. If  $3D\tau/R^2 = 1$  for a cell with  $D = 0.9 \times 10^{-9} \text{ m}^2/\text{s}$  and  $R = 0.59 \text{ mm}$  (the values of oocytes described herein),  $\tau$  for that cell would be 127 s. That lifetime is longer than the lifetime reported herein for real cells, but still, under those conditions,  $P_d$  would be 28% greater than  $P'_d$ .

Other investigators have described intracellular motion in terms of an “unstirred layer” (Finkelstein, 1987; Zhang and Verkman, 1991). This idea is based on the observation that, when a compartment is actively stirred, water motion gradually decreases as water nears the compartment border (membrane). At the border, water motion is due solely to diffusion. This behavior is idealized for permeability measurements by assuming perfect mixing up to a certain distance  $\delta$  from the membrane surface. Mixing in that layer is

assumed to be due to diffusion only. This treatment is flawed because no mixing mechanism that significantly affects water motion is present in oocytes. Water motion throughout the oocyte has been shown to be due exclusively to diffusion (Sehy et al., 2002a). An unstirred layer may exist outside cells. For the purposes of this study, the extracellular unstirred layer is assumed to be negligibly thin.

### The $P_f/P_d$ ratio

In the introduction, it was stated that  $P_f/P'_d$  may be  $>1$  if intracellular displacement is not fast relative to water movement across the membrane. In that case,  $P'_d$  underestimates true diffusional permeability  $P_d$ . In this report, the dependence of  $P'_d$  on  $D$  was discussed in depth, and  $P_d$  was found to be  $39 \pm 6\%$  greater than  $P'_d$ . In a 1991 study, the ratio  $P_f/P'_d$  was reported to be 2.4 for the oocyte (Zhang and Verkman, 1991). Substituting  $P_d$  for  $P'_d$ , the ratio  $P_f/P_d$  becomes 1.7, smaller but still somewhat greater than 1. This result could be due to at least two factors. First, the model for  $P_d$  described herein may be overly simple. For example, a single value for  $D$  was used to describe intracellular water diffusion even though the water diffusion constant is different in different volumes of the cell. Second, a  $P_f/P_d$  ratio greater than 1 may indicate the presence of water channels in the membrane as discussed in the introduction.

### CONCLUSION

Magnetic resonance was shown to provide a unique method of measuring true diffusional membrane permeability  $P_d$ . Magnetic resonance spectroscopy was used to monitor oocyte membrane water exchange with better temporal resolution and SNR than previously described methods. Magnetic resonance imaging can be used to determine cell volume and intracellular water ADC. Together, this information permits direct determination of  $P_d$ . True diffusional permeability  $P_d$  was found to be  $39 \pm 6\%$  greater than apparent diffusional permeability  $P'_d$ . These results suggest that intracellular water diffusion cannot be ignored in the calculation of diffusional membrane permeability for large cells. For smaller cells such as the erythrocyte, intracellular water diffusion should have little effect on the measurement of intracellular lifetime or calculation of diffusional membrane permeability.

The authors thank James Quirk for interesting discussions. This work was supported by National Institutes of Health grants NS35912 and R24-CA83060.

### REFERENCES

- Barry, P. H., and J. M. Diamond. 1984. Effects of unstirred layers on membrane phenomena. *Physiol. Rev.* 64:763–872.

- Carslaw, H. S., and J. C. Jaeger. 1959. *Conduction of Heat in Solids*. 2nd Ed. Clarendon Press, Oxford, U.K. 230–237.
- Crank, J. 1975. *The Mathematics of Diffusion*. 2nd Ed. University Press, Oxford, U.K. 89–103.
- Finkelstein, A. 1987. Water Movement through Lipid Bilayers, Pores, and Plasma Membranes: Theory and Reality. Wiley-Interscience, New York. 38–41.
- Haglund, B., and C. A. Loeffler. 1969. Water diffusion and water permeation in eggs from three Anuran species. *J. Cell Physiol.* 73:69–80.
- Herbst, M. D., and J. H. Goldstein. 1989. A review of water diffusion measurement by NMR in human red blood cells. *Am. J. Physiol. Cell Physiol.* 256:C1097–C104.
- Iserovich, P., K. Kuang, T. Chun, and J. Fischbarg. 1997. A novel method to determine the diffusional water permeability of oocyte plasma membranes. *Biol. Cell.* 89:293–297.
- Koefoed-Johnsen, V., and H. H. Ussing. 1953. The contribution of diffusion and flow to the passage of D<sub>2</sub>O through living membranes. Effect of neurohypophyseal hormone on isolated anuran skin. *Acta Physiol. Scand.* 28:60–76.
- Lovtrup, S. 1963. On the rate of water exchange across the surface of animal cells. *J. Theor. Biol.* 5:341–359.
- Mild, K. H. 1972. Diffusion exchange between a membrane-bounded sphere and its surrounding. *Bull. Math. Biophys.* 34:93–102.
- Prescott, D. M., and E. Zeuthen. 1952. Comparison of water diffusion and water filtration across cell surfaces. *Acta Physiol. Scand.* 28:77–94.
- Sehy, J. V., J. J. Ackerman, and J. J. Neil. 2001. Water and lipid MRI of the *Xenopus* oocyte. *Magn. Reson. Med.* 46:900–906.
- Sehy, J. V., J. J. H. Ackerman, and J. J. Neil. 2002a. Apparent diffusion of water, ions, and small molecules in the *Xenopus* oocyte is consistent with Brownian displacement. *Magn. Reson. Med.* 48:42–51.
- Sehy, J. V., J. J. H. Ackerman, and J. J. Neil. 2002b. Evidence that both “fast” and “slow” water ADC components arise from the intracellular space. *Magn. Reson. Med.* In press.
- Sehy, J. V., J. J. H. Ackerman, and J. J. Neil. 2002c. Intracellular water ADC decrease following a reduction in cell ATP levels. *Proc. ISMRM.* 1149.
- Smith, L. D., W. L. Xu, and R. L. Varnold. 1991. Oogenesis and oocyte isolation. *Methods Cell Biol.* 36:45–60.
- Snaar, J. E. M., and H. Van As. 1992. Probing water compartments and membrane permeability in plant cells by <sup>1</sup>H NMR relaxation measurements. *Biophys. J.* 63:1654–1658.
- Stejskal, E. O., and J. E. Tanner. 1965. Spin diffusion measurements: spin echoes in the presence of time-dependent field gradients. *J. Chem. Phys.* 42:288–292.
- Verkman, A. S. 2000. Water permeability measurement in living cells and complex tissues. *J. Membr. Biol.* 173:73–87.
- Waldeck, A. R., M. H. Nouri-Sorkhabi, D. R. Sullivan, and P. W. Kuchel. 1995. Effects of cholesterol on transmembrane water diffusion in human erythrocytes measured using pulsed field gradient NMR. *Biophys. Chem.* 55:197–208.
- Zhang, R. B., and A. S. Verkman. 1991. Water and urea permeability properties of *Xenopus* oocytes: expression of mRNA from toad urinary bladder. *Am. J. Physiol. Cell Physiol.* 260:C26–C34.